

Chapter 7

Tower Cross Arm Numerical Analysis

In this section the structural analysis of the test tower cross arm is done in Prokon and compared to a full finite element analysis using Ansys. This is done in order to establish how the members in the structural analysis should be constrained and modeled in order to achieve realistic member forces. It will be shown that modeling the tower cross arm members based on the conventional method of using pinned connections is not adequate for tubular transmission structures. Connection eccentricity has a significant effect on the selection of member sizes and connection design.

The Prokon Frame Analysis software is a finite element package that is used to represent the tower cross arm with three dimensional beam elements. This is the preferred method of designing truss type structures where truss members are usually only subjected to compression or tension loads. Bending moments will also be accounted for in the tubular transmission tower due to connection eccentricities. The local stiffness of each beam element is then assembled in a global stiffness matrix from which various results can be extracted. The Ansys finite element software is used to take the actual cross arm CAD model and mesh it with many discrete elements. In this cross arm model there were 38180 elements. In the Ansys FEA model a lot more attention to connection detail has to be given in order to replicate realistic connection behaviour. It can thus be seen that there are distinct advantages to use Prokon for the commercial application of tower design. Typical advantages are that the structural models are much quicker to assemble and edit, less pre-processing time is required and it is solved very quickly.

7.1 Structural modeling of the tower cross arm

The first structural model of the tower cross arm (figure 7.2) is done in Prokon. The supports are fully fixed and the conductor attachment point is pinned. This would also be the conventional method when designing structures with angular members. The connections will be detailed in order to minimize the effect of secondary bending moments.

The second structural model (figure 7.3) is also done in Prokon. The supports are fully fixed and the conductor attachment point is assembled with rigid links in order to generate additional bending moments at the supports resulting from the eccentricities at the conductor attachment point and the $D/2$ effect of the CHS member.

The third structural model (figure 7.4) is the finite element model. A 3D parasolid of the tower cross arm was imported into the FEA software. In order to reduce computation time, the model was converted into shell elements. Shell elements were used due to their applicability to long slender members with constant thickness. The mesh control was set to standard mechanical, program controlled and the size was limited between 5mm to 10mm. An evenly distributed quad mesh was generated (figure 7.5). Depending on the required output of the results, the mesh should be adjusted accordingly. For example, in this analysis, the reaction forces and bolt connection forces are more important than detailed stress analysis results, and the mesh size could have been program controlled in order to reduce computation time. The mesh size could also be refined around bolt holes or where expected stress concentrations could occur.

A revolute joint was used to constrain the bolt holes (figure 7.6). This type of joint constrains the holes relative to each other for all degrees of freedom except rotation along the axial direction of the two holes (z-direction). A reaction probe can be placed on each bolt connection; this will allow the engineer to evaluate the loads in each bolt separately. The probe will display the reaction forces which can then be viewed graphically (see figure 7.7 and figure 7.8). High stress gradients could occur around the perimeter of bolt joints (figure 7.9), it will thus be useful to use the reaction probe tool to evaluate the actual forces to determine if these stress are of concern.

A lot more is left to be said about the constraints, analysis type (linear

vs. nonlinear), method of applying loads, including dynamic loads from conductor vibration and detailed bolt modeling. This will however be reserved for future studies on tubular transmission tower cross arms. These factors will however not affect this analysis seeing that the required results are more focused on reaction forces and moments which is affected by the overall system rather than localized material and connection behaviour.

Once the models have been setup, four different load cases were applied to the cross arm. These loads also represent the actual loads that will be applied to the test structure. Description of load cases can be found in previous chapter (see figure 6.3):

- high transverse - compression (table 7.1)
- high transverse - tension (table 7.2)
- cascade failure (table 7.3)
- broken conductor (table 7.4)

In Prokon model 1, the loads were applied to node 4 as seen in figure 7.2. In Prokon model 2, the loads were applied to the ends of the two rigid links indicated by node 8 and node 9. Figure 7.5 shows six red dots (bolt holes) where the loads were applied. These six holes also represent the bracket attachment holes for supporting the insulator set which in turn supports the conductor.

Figure 7.1 shows how the load cells were connected to the tip of the test tower. The conductor attachment plates can also be seen with shackles that transfers the loads into the main members of the cross arm. Figure 8.1 shows the tower fixed to the test bed.

The support reactions (forces and moments) were tabulated and compared (table 7.1 - 7.4). The results show, the left hand, right hand and top support as seen in the page layout. Throughout the tabulated results, it can be seen that FEA results compare very well with Prokon Model 2 (figure 7.3). This indicates that it is necessary to model all eccentricities into the structural model in order to achieve realistic results. This model also proves with the aid of the interaction equation (equation 7.1) that the additional bending moments that are created as a result of connection eccentricities has a significant effect on the selection of member sizes.



Figure 7.1: Photo showing the attachment of the load cells on the test structure cross arm.

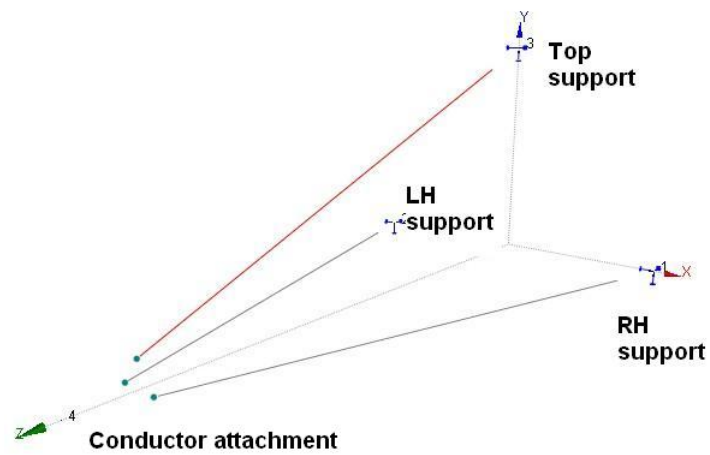


Figure 7.2: Prokon model 1: Tripod cross arm model - pinned. This cross arm has three main members that are fixed at the support and pinned at the conductor attachment end.

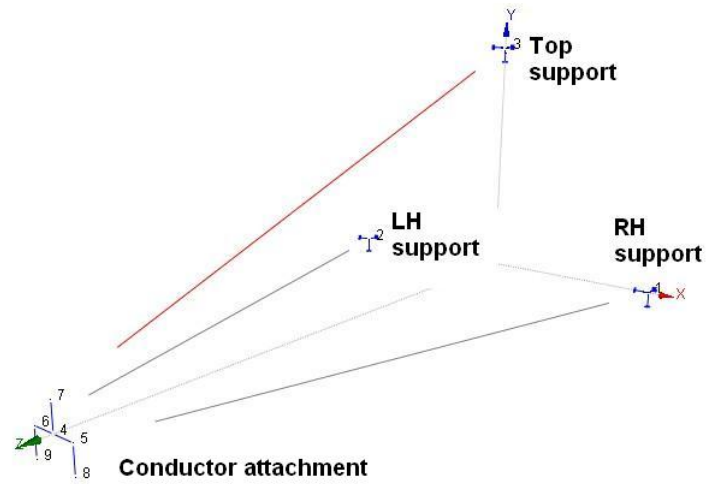


Figure 7.3: Prokon model 2: Improved cross arm model with specific end connection detail. The cross arm model consist of three main members that are fixed at the support and the conductor attachment end is more detailed with rigid links. Rigid represents only load transferring and not a structural member.

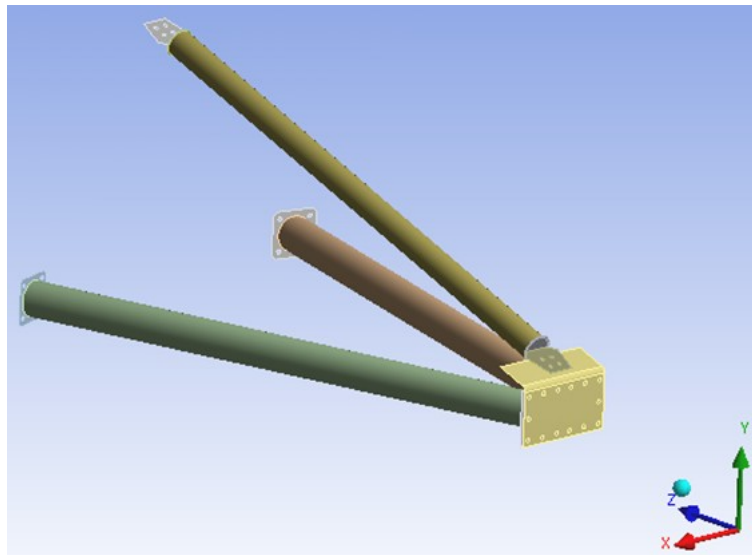


Figure 7.4: Finite element model of 3D cross arm.

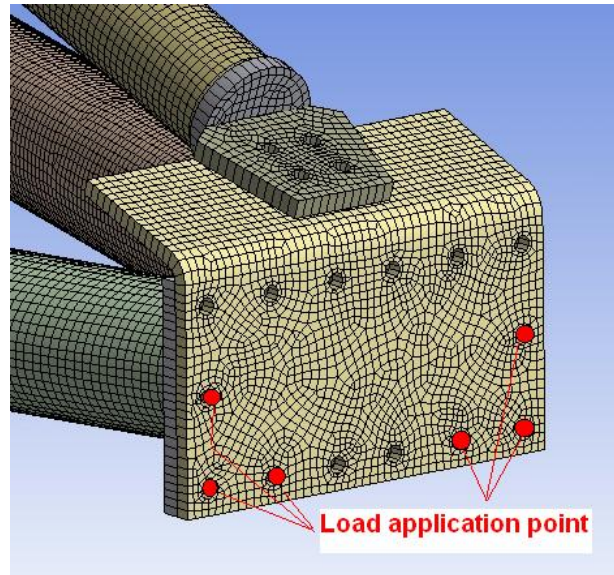


Figure 7.5: Cross arm mesh control display after mesh refinement.

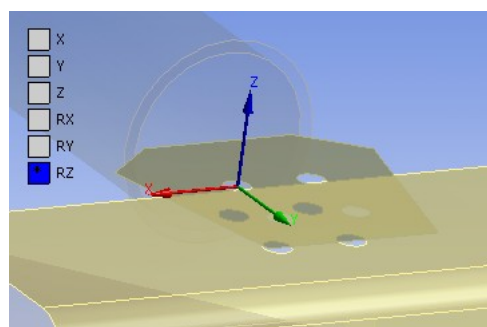


Figure 7.6: Revolute joint (Top 1A) indicating only rotation about the z-axis is permitted.

LC 1 - High Transverse, Compression				
Support	Reaction	Prokon model 1	Prokon model 2	FEA
Right hand support	$M_x(kNm)$	3.83	11.75	10.6
	$M_y(kNm)$	0.14	0.52	1.47
	$M_z(kNm)$	1.15	2.34	2.55
	$R_x(kN)$	43.59	37.12	35.97
	$R_y(kN)$	1.53	6.5	7.5
	$R_z(kN)$	145.5	143.04	141.0
Left hand support	$M_x(kNm)$	1.82	11.75	10.60
	$M_y(kNm)$	0.14	0.52	1.47
	$M_z(kNm)$	1.15	2.34	2.55
	$R_x(kN)$	43.59	37.12	35.9
	$R_y(kN)$	1.53	6.5	7.5
	$R_z(kN)$	145.5	143.04	141.0
Top support	$M_x(kNm)$	1.34	1.38	1.26
	$M_y(kNm)$	0.0	0.0	0.0
	$M_z(kNm)$	0.0	0.0	0.0
	$R_x(kN)$	0.0	0.0	0.18
	$R_y(kN)$	76.94	66.99	65.1
	$R_z(kN)$	191.01	186.08	182.0

Table 7.1: Load case 1: High transverse wind. Cross arm in compression, reaction forces and moment reactions at cross arm support.

LC 2 - High transverse wind. Tension				
Support	Reaction	Prokon model 1	Prokon model 2	FEA
Right hand support	$M_x(kNm)$	3.04	13.83	13.14
	$M_y(kNm)$	0.05	0.11	0.89
	$M_z(kNm)$	0.91	3.58	3.79
	$R_x(kN)$	13.92	7.74	8.65
	$R_y(kN)$	1.22	10.89	12.02
	$R_z(kN)$	46.45	29.83	27.83
Left hand support	$M_x(kNm)$	3.04	13.83	13.14
	$M_y(kNm)$	0.05	0.11	0.89
	$M_z(kNm)$	0.91	3.58	3.79
	$R_x(kN)$	13.92	7.74	8.65
	$R_y(kN)$	1.22	10.89	12.02
	$R_z(kN)$	46.45	29.83	27.83
Top support	$M_x(kNm)$	1.03	1.73	1.19
	$M_y(kNm)$	0.0	0.0	0.0
	$M_z(kNm)$	0.0	0.0	0.0
	$R_x(kN)$	0.0i	0.0	0.03
	$R_y(kN)$	77.57	58.22	55.94
	$R_z(kN)$	192.89	159.66	156.0

Table 7.2: Load case 2: High transverse wind- Cross arm in tension, reaction forces and moment reactions at cross arm support.

LC 3 - Cascade failure				
Support	Reaction	Prokon model 1	Prokon model 2	FEA
Right hand support	$M_x(kNm)$	3.83	9.97	10.01
	$M_y(kNm)$	1.33	8.78	7.16
	$M_z(kNm)$	1.15	5.14	5.93
	$R_x(kN)$	73.57	66.71	65.5
	$R_y(kN)$	1.72	6.05	7.91
	$R_z(kN)$	243.45	224.66	221.0
Left hand support	$M_x(kNm)$	3.83	16.96	14.42
	$M_y(kNm)$	1.55	9.54	8.31
	$M_z(kNm)$	1.15	0.96	0.47
	$R_x(kN)$	6.24	12.79	13.05
	$R_y(kN)$	1.72	12.0	11.57
	$R_z(kN)$	18.74	16.85	18.22
Top support	$M_x(kNm)$	1.36	1.67	1.29
	$M_y(kNm)$	0.48	0.54	1.13
	$M_z(kNm)$	0.19	0.62	0.9
	$R_x(kN)$	0.19	0.49	1.45
	$R_y(kN)$	81.76	67.34	64.73
	$R_z(kN)$	202.72	185.81	180.0

Table 7.3: Load case 3: Cascade failure - Combination of tension and compression loads (Large overturning moment at tower base), reaction forces and moment reactions at cross arm support .

LC 4 - Broken conductor				
Support	Reaction	Prokon model 1	Prokon model 2	FEA
Right hand support	$M_x(kNm)$	1.82	0.95	2.82
	$M_y(kNm)$	2.19	14.13	11.91
	$M_z(kNm)$	0.54	4.7	6.15
	$R_x(kN)$	79.16	75.66	74.13
	$R_y(kN)$	0.73	0.5	2.79
	$R_z(kN)$	260.96	240.90	237.0
Left hand support	$M_x(kNm)$	1.82	11.87	9.05
	$M_y(kNm)$	2.3	14.51	12.64
	$M_z(kNm)$	0.54	1.83	3.09
	$R_x(kN)$	45.54	48.56	48.79
	$R_y(kN)$	0.73	8.8	6.79
	$R_z(kN)$	148.72	136.46	135.00
Top support	$M_x(kNm)$	0.63	0.77	0.64
	$M_y(kNm)$	0.75	0.84	1.78
	$M_z(kNm)$	0,3	0.97	1.43
	$R_x(kN)$	0.3	0.77	2.07
	$R_y(kN)$	39.55	32.7	31.41
	$R_z(kN)$	98.55	90.45	88.09

Table 7.4: Load case 4: Broken conductor- Tower under twisting action, reaction forces and moment reactions at cross arm support.

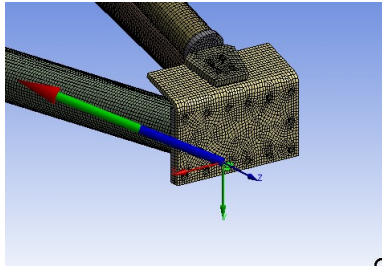


Figure 7.7: Reaction forces on revolute joint.

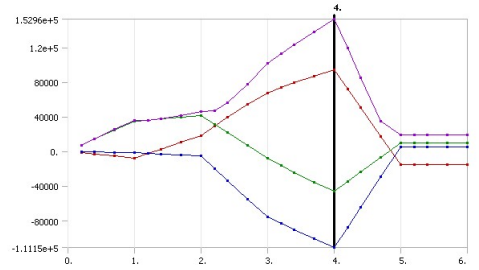


Figure 7.8: Graphical representation of reaction forces at a joint probe.

$$\frac{Cu}{Cr} + \frac{Mu}{Mr} \leq 1.0 \quad (7.1)$$

From LC1, Right hand support, the usage of the lower cross arm member is 31% for Prokon model 1. When comparing that to Prokon model 2, the usage is increased to 54%. This is an increase of 23% which is substantial and should not be overlooked or ignored. By doing so will result in structural members which are not adequately designed to resist axial loads and bending moments that will result in member failure when tested.

To conclude, the results show that there is good agreement between the FEA analysis and the Prokon analysis (Prokon model 2). This shows that a Prokon model can be used to design the cross arm, provided that *fixed connections* are used in the conductor attachment point and members are realistically spaced with rigid links.

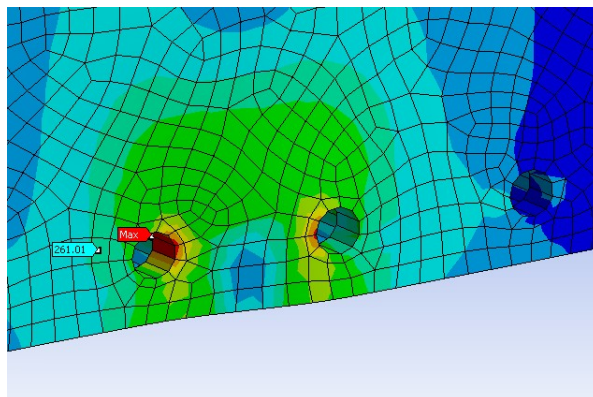


Figure 7.9: High stress gradient around hole joint.